



## Preparation, characterization and performance of PVDF/ $\text{Al}_2\text{O}_3$ , $\text{TiO}_2$ and clay membrane for removal of toxic metals

Mohsen Hesavi<sup>a</sup>, Ehsan Derikvand<sup>a</sup>, Mohsen Solimani Babarsad<sup>a,\*</sup>, Mahmood Shafaei Bejestan<sup>b</sup>, Mojgan Zendehtel<sup>c</sup>

<sup>a</sup>Department of Water Science, Shoushtar Branch, Islamic Azad University, Shoushtar, Iran, email: Mohsen.solb@gmail.com (M.S. Babarsad)

<sup>b</sup>Department of Water Engineering, Faculty of Water and Environmental, Shahid Chamran University, Ahvaz, Iran

<sup>c</sup>Department of Chemistry, Faculty of Science, Arak University, Arak, 38156-8-8349, Iran

Received 28 July 2023; Accepted 5 October 2023

### ABSTRACT

In this study, two membranes including polyvinylidene fluoride (PVDF) and PVDF/ $\text{Al}_2\text{O}_3$ ,  $\text{TiO}_2$ , and clay were synthesized. Organic–inorganic composite membrane is formed by nano-sized  $\text{Al}_2\text{O}_3$ ,  $\text{TiO}_2$  and clay particles that uniformly dispersed in the polyvinylidene fluoride (PVDF) solution and then casting films. The structure of membranes was characterized by several techniques such as scanning electron microscopy, Fourier-transform infrared spectroscopy (FT-IR) and thermogravimetric analysis. The results showed that the  $\text{Al}_2\text{O}_3$ ,  $\text{TiO}_2$  and clay nanoparticles were incorporated into the pores and onto the surface of PVDF, and more uniform hybrid structure was obtained. The FT-IR spectra revealed that the weak physical interaction played role in the construction of hybrid membranes. Compared with the PVDF film, the permeability and antifouling performance of hybrid membrane was improved. In addition, this membrane utilized for removal toxic metals of industrial wastewater. The results showed that, the PVDF/ $\text{Al}_2\text{O}_3$ ,  $\text{TiO}_2$ , clay hybrid membrane has better decrees electrical conductivity of wastewater, and it showed better adsorption properties for lead and arsenic ions, which was rarely reported. The most uptake % of lead ion were 88.5% at pH 4 and 91.0% for arsenic ion at pH 7. The important point of this high-capacity membrane for absorbent toxic cations is the using of low amounts of nanoparticles that are low cost and greatly favoured in view of green chemistry.

**Keywords:** Organic–inorganic composite; Polyvinylidene fluoride; Nano-sized  $\text{Al}_2\text{O}_3$ ;  $\text{TiO}_2$  particles; Electrical conductivity; Toxic metals

### 1. Introduction

Increasing attention has recently been paid to the use of hybrid materials. These materials could combine basic properties of organic and inorganic materials and suggestion-specific advantages for the preparation of artificial membranes with excellent separation performances, good thermal and chemical stability and adaptability to harsh environments, as well as membrane forming ability. As new

membrane materials, organic–inorganic hybrid materials have attracted more attention [1–6].

Polyvinylidene fluoride (PVDF) is one of the most attractive polymer materials in the water treatment industry due to its excellent chemical resistance, thermal stability, low toxicity, and good mechanical properties [6,7]. Nevertheless, its hydrophobic characteristic, which often leads to severe membrane fouling and a decline in permeability, limits its application in water treatment. Several strategies to improve

\* Corresponding author.

the hydrophilicity of PVDF membranes have therefore been investigated such as physical blending, chemical grafting, and surface modification [6]. Recently, studies on the modification of PVDF by blending polymer with inorganic materials have been considered. Inorganic materials that can be blended with PVDF include aluminum oxide ( $\text{Al}_2\text{O}_3$ ) [6,8], titanium dioxide ( $\text{TiO}_2$ ) [9], zirconium dioxide ( $\text{ZrO}_2$ ) [10], and silica ( $\text{SiO}_2$ ) [11,12]. Initially, most of these modifications are the addition of nanoparticles to the casting solutions to prepare the hybrid membranes. To promote the dispersion of the organic components in polymers, a sol–gel process was used to grow the inorganic phase in the polymer solution. The sol–gel technique has provided new opportunities for the preparation of organic–inorganic materials, which allows the formation of the inorganic framework under mild conditions and the incorporation of minerals into polymers, resulting in increased chemical, mechanical, and thermal stabilities without obviously decreasing the properties of the polymers [13,14].

Toxic metal (e.g., Pb, Cd, Hg, Zn, Cu, Cr, Ni, As) ions from industrial processes are of special importance because they produce chronic poisoning in aquatic environments. More emphasized environmental regulations on the discharge and release of toxic metals require developing various technologies for their removal from polluted streams such as industrial wastewater, landfill leachate, mine waters and groundwater. The separation of toxic metal ions using immobilized materials such as novel sorbents and membranes with doped ligands, due to their high selectivity and removal efficiency, increased stability, and low energy requirements, is promising for application to improve the environmental quality [15].

The hydrophilicity of the membranes and their porous structure play an essential role in membrane separation processes. To obtain high permeability, the high surface porosity and good pore structure of membranes are essential. The asymmetric membrane is the most ideal one for this object. Among all organic macromolecule polymer materials, PVDF is one of the excellent materials that can form asymmetric membranes [16]. Different industrial wastes, particularly such as those from mining, electro-plating, lead smelting metal finishing industries, discharge significant amounts of heavy metals in various forms. The concentration of these metals in wastewater may therefore rise to a level that can be hazardous to livestock. Lead is of particular interest because of its toxicity and its widespread presence in the environment [17–20].

Treatment processes for toxic metals removal from water and wastewater through adsorption or ion exchange were recently studied. Park et al. [21] used sargassum for the removal of lead and cadmium ions from water. Petruzzelli et al. [22] and Faghihian et al. [23] used clinoptilolite in the sodium form to removal of lead in battery and nuclear wastewater, respectively. Vecchio et al. [24] studied the removal of Cu, Pb and Cd ions by biosorption on bacterial cells. Srivastav et al. [25] used the aquatic plants and chabazite as a natural zeolite exchanger for removal of lead ions from water. Namasivayam and Ranganathan [26] used iron III/chromium III hydroxide as an adsorbent. Laumakis et al. [27] used fly ash subgrades for the removal of lead ions from wastewater.

Studies on the immobilized material showed that the removal efficiency of toxic metal ions depends on the chemical nature of the materials and the solution conditions like ion concentration, pH of the medium and presence of competing ions. Different types of forces and interactions including hydrogen bonding, electrostatic interaction, surface complexation and van der Waal forces, ion exchange, and so forth, are responsible for the removal of toxic metal ions from waste streams using immobilized materials.

In this work, PVDF and PVDF/ $\text{Al}_2\text{O}_3$ ,  $\text{TiO}_2$  and clay hybrid membranes were prepared. The aim was to investigate the feasibility of using the new type of PVDF hybrid membranes mixed with inorganic additives like  $\text{Al}_2\text{O}_3$ ,  $\text{TiO}_2$ , and clay as a highly efficient absorbent for the removal of toxic metals from real industrial wastewater. The Fourier-transform infrared spectroscopy (FT-IR), scanning electron microscopy (SEM), energy-dispersive X-ray spectroscopy (EDS) and thermogravimetric analysis (TGA) were used to characterize of the membranes. Then, the absorption efficiency of lead and arsenic ions by the better membrane was investigated. The effect of contact time, pH and concentration of lead and arsenic ions on the uptake % was also studied. The effect of different amounts of  $\text{Al}_2\text{O}_3$ ,  $\text{TiO}_2$ , clay nanoparticles on membrane structure and properties were investigated.

## 2. Experimental

### 2.1. Materials and instruments

The polyvinylidene fluoride (PVDF) and N,N-dimethylformamide (DMF, 0.99%, reagent) used were purchased from Alfa Aesar and Merck, respectively.  $\text{Al}_2\text{O}_3$  and  $\text{TiO}_2$  particles with nano-size, lead nitrate and arsenic nitrate salts used were purchased from Merck. FT-IR spectra were recorded on a Galaxy Series FT-IR 5000 Spectrometer. Field emission scanning electron microscope (FESEM) photographs of the samples were obtained using a Zeiss Sigma VP FESEM Instrument. The instrument used for determination of lead and arsenic ions concentration was a Perkin Elmer 2380 Atomic Absorption Spectrometry. The pH meter model 744 Metrohm and electrical furnace 1,200°C were also used.

### 2.2. Membranes preparation

#### 2.2.1. PVDF membrane (M1)

At first, the polyvinylidene fluoride (1.0 g) was dissolved in 20 mL of N,N-dimethylformamide solvent at 75°C with strong stirring. Then at the same temperature, the solution was degassed for 24 h. The resulting liquid was placed on a glass plate for filming. Finally, the resulting polymer membrane was placed in deionized water for 24 h, to separate the solvent and remaining pores and to keep it dry [28,29].

#### 2.2.2. PVDF/ $\text{Al}_2\text{O}_3$ , $\text{TiO}_2$ and clay hybrid membranes (M2, M3, M4 and M5)

All polymer membranes (M2, M3, M4 and M5 according to Table 1) were synthesized by phase-inversion method. Firstly, for each of the membranes, nanoparticles contain  $\text{Al}_2\text{O}_3$ ,  $\text{TiO}_2$  and clay dissolved in N,N-dimethylformamide

Table 1  
Components of polymer membranes (M1, M2, M3, M4 and M5)

Sample	Weight (g)			
	TiO <sub>2</sub>	Al <sub>2</sub> O <sub>3</sub>	Clay	PVDF
M1	–	–	–	1.00
M2	0.01	0.01	–	1.00
M3	0.01	0.01	0.01	1.00
M4	0.02	0.02	0.02	1.00
M5	0.01	0.008	0.006	1.00

solvent at 75°C with strong stirring. The resulting mixture was placed in the ultrasonic system for 15 min at 20°C. Then polyvinylidene fluoride (1.0 g) was added to that, to obtain an optimal dispersion of the particles in polymer solutions. The above mixture was stirred for 24 h at 75°C to obtain homogenous casting solution and degassed. Then it was placed in the electrical furnace for 24 h at 560°C. The resulting polymer membranes was placed on a glass plate for filming. Finally, each of the resulting organic–inorganic membranes was placed in deionized water for 24 h, to separate the solvent and remaining pores [28–31].

### 2.3. Membranes performance

The electrical conductivity (EC) and pH of each of the wastewater samples taken were measured. Then, to achieve the optimal membrane, the PVDF and PVDF/Al<sub>2</sub>O<sub>3</sub>, TiO<sub>2</sub> and clay membranes were placed separately in the glass column and concentrated sodium chloride solution was passed through it (continues system).

Then, in order to evaluate the adsorption efficiency of heavy metals with the superior membrane, the standard solution of 4.0 and 10.0 mg/L of lead and arsenic ions was prepared at different pH. The membrane was then placed in a glass column and the prepared solution was passed through it at different times (continuous method).

## 3. Results and discussion

The M5 membrane by low dosage of nanoparticles has been high efficiency performance as an absorbent. Analyses related to this membrane were investigated.

### 3.1. FT-IR analysis

FT-IR analysis was employed to investigate the composites of the synthesized membranes. The FT-IR spectra obtained are shown in Fig. 1. Also, the results are observed in Table 2. In the case of PVDF membrane (M1), as shown in Fig. 1a, the bands of 3020 and 2970 cm<sup>-1</sup> were assigned to the non-symmetrical and symmetrical stretching vibration of CH<sub>2</sub> groups; the band of 1,400 cm<sup>-1</sup> was caused by the deformed vibration of CH<sub>2</sub> groups; the band at 1,180 cm<sup>-1</sup> was associated with the stretching vibration of CF<sub>2</sub> groups; the bands of 607, 757, 838 and 877 cm<sup>-1</sup> were characteristic of amorphous phase and phase PVDF [28–37]. In the case of PVDF/Al<sub>2</sub>O<sub>3</sub>, TiO<sub>2</sub>, clay membrane (M5), as shown in Fig. 1b, apart from the characteristic absorption

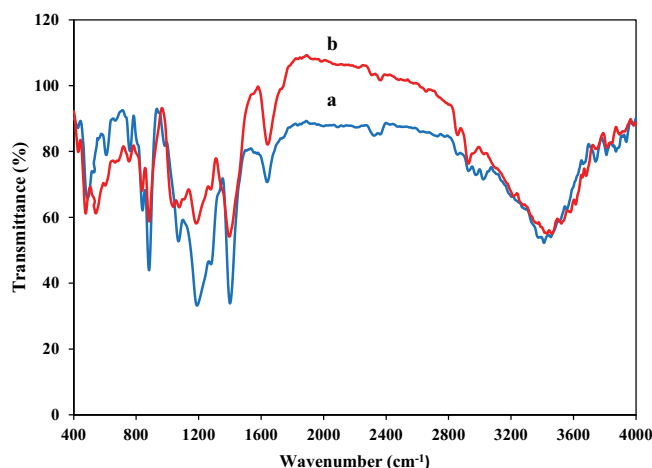


Fig. 1. Fourier-transform infrared spectra of PVDF membrane (M1) (a) and PVDF/Al<sub>2</sub>O<sub>3</sub>, TiO<sub>2</sub>, clay hybrid membrane (M5) (b).

Table 2  
FT-IR spectra of membranes

Sample	Vibrations (cm <sup>-1</sup> )		
	CF <sub>2</sub>	CH <sub>2</sub> –CF <sub>2</sub>	CH <sub>2</sub>
PVDF (M1)	494; 531; 610; 796; 883; 1,284	841; 1,072; 1,192	1,400
PVDF/Al <sub>2</sub> O <sub>3</sub> , TiO <sub>2</sub> , clay (M5)	478; 540; 752; 883; 1,276	841; 1,076; 1,184	1,396

bands of PVDF and Al<sub>2</sub>O<sub>3</sub>, TiO<sub>2</sub>, clay, little change could be observed. The presence of the absorption band at 1,596 cm<sup>-1</sup>, ascribed to the stretching mode of Al–O–Al, suggested the existence of Al<sub>2</sub>O<sub>3</sub> in the hybrid membrane [36]. No other band was founded, which proved that the physical interaction played role in the construction of PVDF/Al<sub>2</sub>O<sub>3</sub>, TiO<sub>2</sub>, clay hybrid membranes.

### 3.2. SEM-EDS analysis

Fig. 2 shows the SEM images of TiO<sub>2</sub> (a) and Al<sub>2</sub>O<sub>3</sub> nanoparticles (b). TiO<sub>2</sub> nanoparticles are cubic in shape and about 21–25 nm in particle size. Also, the shape of Al<sub>2</sub>O<sub>3</sub> nanoparticles is semi spherical and their size is about 50–60 nm.

The morphology of the membranes surface were examined by SEM. Fig. 3a and b show the SEM images of the PVDF membrane (M1) surface, that the structure contains large holes with non-uniform distribution. Fig. 3c–f shows the SEM images of PVDF/Al<sub>2</sub>O<sub>3</sub>, TiO<sub>2</sub>, clay membrane (M5) surface and cross-section. It can be seen that the micropores were distributed on membrane surfaces with different additions of Al<sub>2</sub>O<sub>3</sub> and TiO<sub>2</sub>, clay particles. Fig. 3c–f shows a smaller pore size and higher porosity. A homogeneous with uniformly sized pore membrane was obtained, when the content of Al<sub>2</sub>O<sub>3</sub>, TiO<sub>2</sub>, clay was present.

It is apparent that the pores are uniformly dispersed along the entire membrane surface and the cross-section structure of the composite membrane is typical asymmetric

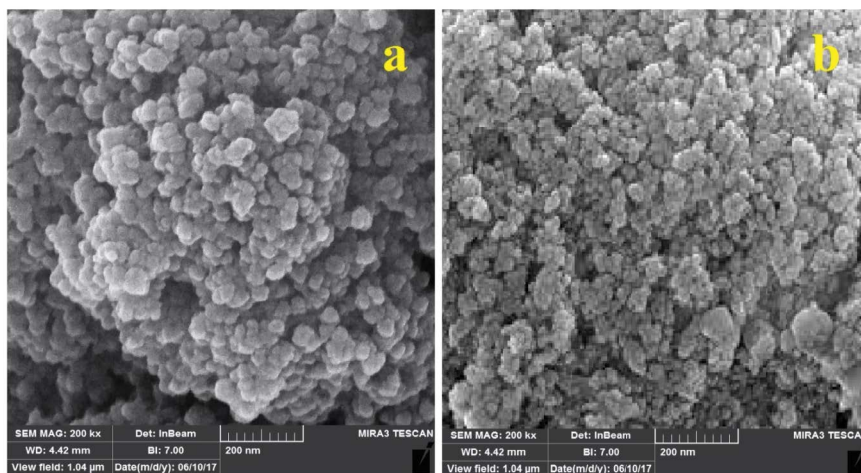


Fig. 2. Scanning electron microscopy images of TiO<sub>2</sub> (a) and Al<sub>2</sub>O<sub>3</sub> nanoparticles (b).

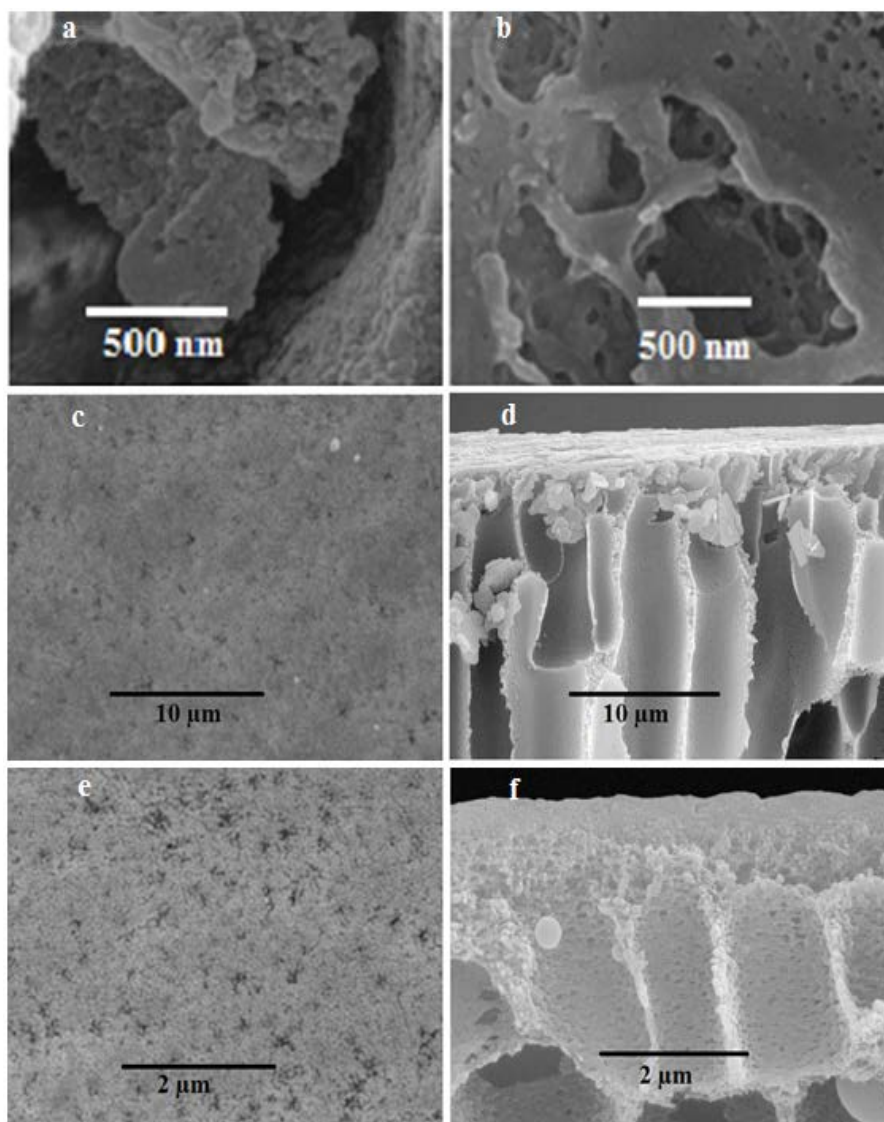


Fig. 3. Scanning electron microscopy images of PVDF membrane (a,b) and PVDF/Al<sub>2</sub>O<sub>3</sub>, TiO<sub>2</sub> clay membrane (c-f).

morphology. This indicates that the addition of  $\text{Al}_2\text{O}_3$ ,  $\text{TiO}_2$  and clay particles cannot affect the structures of the surface and cross-section. Therefore, the mechanism of the PVDF membrane formation is not altered by the addition of inorganic particles. Performances of modified membranes are influenced by the condition of nano-sized particulars distributing.

EDS method in Fig. 4 confirms the presence of Ti, Al, O related to  $\text{TiO}_2$  and  $\text{Al}_2\text{O}_3$  and also C and F in composite, respectively.

### 3.3. TGA analysis

Thermal stability of the PVDF/ $\text{Al}_2\text{O}_3$ ,  $\text{TiO}_2$ , clay membrane was studied by thermogravimetric analysis (TGA) method. The elastic modulus of the membrane increased with increasing weight fraction of nanoparticles. The microhardness value increases with increasing  $\text{Al}_2\text{O}_3$ ,  $\text{TiO}_2$ , clay nanoparticles. In addition, PVDF/ $\text{Al}_2\text{O}_3$ ,  $\text{TiO}_2$ , clay membrane showed higher resistance to thermal degradation compared to PVDF membranes [38]. Moreover, PVDF shows high thermal stability up to  $400^\circ\text{C}$  that increased to about  $600^\circ\text{C}$ – $700^\circ\text{C}$  by adding nanoparticles.

### 3.4. Mechanical properties of organic–inorganic membrane

Particle addition had no obvious effect on the tensile strength of hybrid membranes. These behaviors indicate that adding an appropriate number of nanoparticles to a PVDF solution can improve the membrane's mechanical properties. Particles could act as a cross-linking point in hybrid membranes to link the polymeric chains [28–30] and increase the rigidity of polymeric chains. The rough and hydrophilic surface of the modified membranes was created by combining nanoparticles with polymers to improve the properties of polymer membranes (such as mechanical properties, anti-fouling properties, and antibacterial properties). The porosity of M5 was about 80%. By adding nanoparticles to ( $\text{Al}_2\text{O}_3$ ,  $\text{TiO}_2$  and clay) inside the polymer tissue, the porosity is increased and many smaller holes are formed, which helps to separate the toxic metals [39]. The thickness of PVDF/ $\text{Al}_2\text{O}_3$ ,  $\text{TiO}_2$ , clay membranes was about

50  $\mu\text{m}$ . Adding nanoparticles increased the viscosity of the casting solution, resulting in a thicker skin layer due to the delayed membrane formation mechanism. One major challenge of using intrinsic hydrophilic nanofibers in water separation is their high swelling propensity. We therefore compared the swelling behavior of the surface PVDF and modified PVDF. Dry samples were exposed to saturated water vapor at room temperature for over 70 h. The mass difference before and after water vapor exposure was used to determine water uptake. As shown in Table 3, pristine PVDF nanofibers have a negligible water uptake (swelling) due to a low affinity for water. The modified PVDF nanofibers have water uptake of approximately 10.20%. Results indicate that the modification effectively imparts a hydrophilic surface to the nanofibers while maintaining a low degree of swelling. The wetted PVDF/ $\text{Al}_2\text{O}_3$ ,  $\text{TiO}_2$ , clay membrane is more flexible than PVDF even though it is a much stronger material when it is dry. Overall, swelling is one of the major challenges that limit the ultimate utilization of intrinsically hydrophilic nanofibers in water separations [40].

### 3.5. Membranes performance

#### 3.5.1. Efficiency to reduce of EC

Recently, polymer membranes have been widely used in wastewater treatment [41,42]. In this work, to check the efficiency of the constructed membranes, the EC and pH of several wastewater samples were measured. Subsequently, to achieve the optimal membrane from the PVDF and PVDF/ $\text{Al}_2\text{O}_3$ ,  $\text{TiO}_2$ , clay membranes, each of them was placed separately in the glass column. Then, concentrated sodium chloride solution was passed through it (continues system). According to the results, it was found that the reduction of EC in the case of PVDF membrane (M1) is about 40% less than PVDF/ $\text{Al}_2\text{O}_3$ ,  $\text{TiO}_2$ , clay membrane (M5). In other words, the PVDF/ $\text{Al}_2\text{O}_3$ ,  $\text{TiO}_2$ , clay membrane (M5) was the most efficient in reducing EC and this membrane was chosen to perform the test on the sample taken from the drain (Table 4). The results by error bar for EC content about  $\pm 5 \mu\text{S}$  are given in Table 4.

#### 3.5.2. Efficiency for removal of toxic metals

To evaluate the adsorption efficiency of toxic metals with the PVDF/ $\text{Al}_2\text{O}_3$ ,  $\text{TiO}_2$ , clay membrane (M5), the standard solution of 4.0 and 10.0 mg/L of lead and arsenic ions was prepared at different pH (4, 7 and 9). Then the membrane was placed in a glass column and the prepared solution was passed through it at different times (continuous method). The results by error bars for the concentration of toxic metal of about  $\pm 1 \text{ ppm}$  and EC content about  $\pm 5 \mu\text{S}$  are given in Table 5.

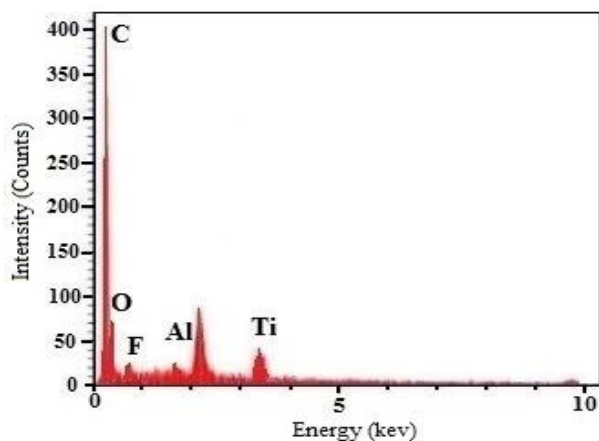


Fig. 4. Energy-dispersive X-ray spectroscopy analysis of M5.

Table 3  
Water uptake of unmodified and modified PVDF

Sample	Water uptake (%)
PVDF (M1)	1.20
PVDF/ $\text{Al}_2\text{O}_3$ , $\text{TiO}_2$ , clay (M5)	10.20

### 3.6. Effect of pH

pH value is an important parameter in the adsorption of toxic metals. The effect of pH (4, 7, and 9) on the uptake % of lead and arsenic ions adsorbed from various

Table 4  
Data of the PVDF/Al<sub>2</sub>O<sub>3</sub>/TiO<sub>2</sub> clay membrane performance investigation

Sample	pH	EC (ohm <sup>-1</sup> ) initial	Time (min)	EC (ohm <sup>-1</sup> ) final	Uptake %
1	7.30	5.91	2	2.18	61.11
			5	2.00	66.16
			10	1.95	67.01
2	7.51	4.33	2	1.60	63.05
			5	1.47	66.05
			10	1.42	67.20
3	7.80	3.05	2	1.12	63.28
			5	1.03	66.23
			10	1.00	67.21
4	7.77	2.55	2	0.94	63.14
			5	0.86	66.27
			10	0.84	67.06
5	7.29	2.58	2	0.95	63.18
			5	0.87	66.28
			10	0.85	67.05
6	7.46	3.81	2	1.40	63.25
			5	1.29	66.14
			10	1.25	67.19

concentrations of lead nitrate (Pb(NO<sub>3</sub>)<sub>2</sub>) solutions and arsenic nitrate (As(NO<sub>3</sub>)<sub>3</sub>) by the PVDF and PVDF/Al<sub>2</sub>O<sub>3</sub>/TiO<sub>2</sub> clay membranes (M5) was investigated. The sequence of lead uptake % (% adsorption) from certain concentrations of lead nitrate solution (4.0 mg/L Pb<sup>2+</sup> or 10.0 mg/L Pb<sup>2+</sup>) and arsenic nitrate solution (4.0 mg/L As<sup>3+</sup> or 10.0 mg/L As<sup>3+</sup>) at different pH by the PVDF/Al<sub>2</sub>O<sub>3</sub>/TiO<sub>2</sub> clay membranes (M5) is shown in Table 5. The uptake % of lead ions increased by decreasing the pH value (in the acidic conditions). The most adsorption of Pb<sup>2+</sup> (88.5%) was observed in pH 4 at a concentration of 10.0 mg/L of lead nitrate solution (Fig. 5).

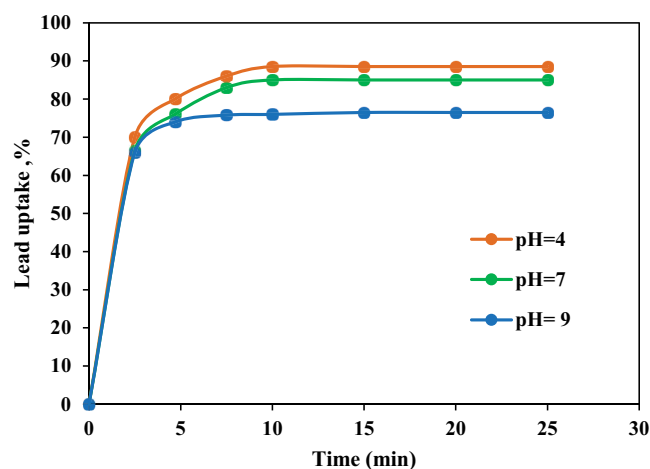


Fig. 5. Effect of contact time on uptake % of lead adsorbed from lead nitrate solution (10.0 mg/L Pb<sup>2+</sup>) by the PVDF/Al<sub>2</sub>O<sub>3</sub>/TiO<sub>2</sub> clay membrane (M5) at pH = 4, 7 and 9.

Table 5  
Results efficiency removal of lead and arsenic ions of wastewaters

Transmembrane time (min)	pH	Pb <sup>2+</sup> concentration (mg/L)			As <sup>3+</sup> concentration (mg/L)		
		Initial	After	Uptake %	Initial	After	Uptake %
2	4	4.00	3.16	21.00	4.00	3.21	19.75
5	4	4.00	2.48	38.00	4.00	2.01	49.75
10	4	4.00	1.48	63.00	4.00	1.41	64.75
2	7	4.00	3.09	22.75	4.00	3.35	16.25
5	7	4.00	2.44	39.00	4.00	2.01	49.75
10	7	4.00	1.19	70.25	4.00	1.02	74.50
2	9	4.00	3.11	22.25	4.00	3.04	24.00
5	9	4.00	2.29	42.75	4.00	2.15	46.25
10	9	4.00	1.03	74.25	4.00	1.27	68.25
2	4	10.00	3.10	69.00	10.00	3.62	63.80
5	4	10.00	2.01	80.00	10.00	2.36	76.40
10	4	10.00	1.14	88.50	10.00	1.25	87.50
2	7	10.00	3.41	66.00	10.00	3.23	67.70
5	7	10.00	2.39	76.20	10.00	2.27	77.30
10	7	10.00	1.47	85.00	10.00	0.92	91.00
2	9	10.00	3.38	66.00	10.00	3.17	68.30
5	9	10.00	2.54	75.00	10.00	2.25	77.50
10	9	10.00	2.45	76.00	10.00	2.17	78.30

Moreover, the uptake % of arsenic ions increased by increasing the pH value (under alkaline conditions). The most adsorption of  $As^{3+}$  (91.0%) was observed in pH 7 at concentrations of 10.0 mg/L of arsenic nitrate solution (Fig. 6).

### 3.7. Effect of contact time

The time effect of adsorption of lead and arsenic ions on the PVDF/ $Al_2O_3$ ,  $TiO_2$  clay membrane (M5) was studied using lead nitrate solution of 4.0 and 10.0 mg/L  $Pb^{2+}$  and arsenic nitrate solution of 4.0 and 10.0 mg/L  $As^{3+}$  at pH = 4, 7 and 9. The effect of contact time and uptake % of Lead and arsenic ions by the PVDF/ $Al_2O_3$ ,  $TiO_2$  clay membrane (M5) is shown in Figs. 5 and 6.

The lead and arsenic uptake % reach equilibrium state about 10 min and remained almost constant between 10 to 25 min. The uptake % curve of lead ions at different times for 10.0 mg/L  $Pb^{2+}$  at pH = 4, 7 and 9 is drawn in

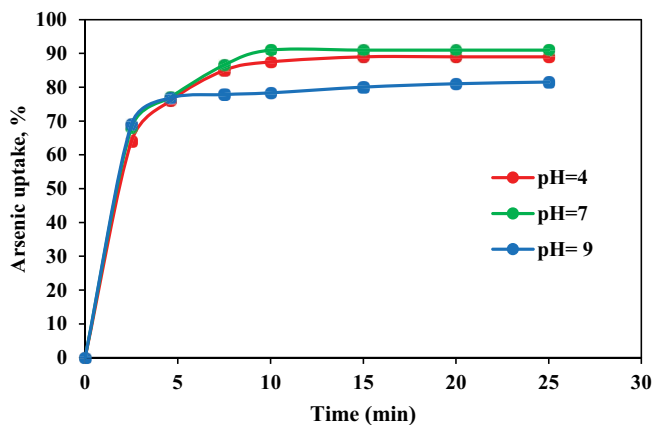


Fig. 6. Effect of contact time on uptake % of arsenic adsorbed from arsenic nitrate solution (10.0 mg/L  $As^{3+}$ ) by the PVDF/ $Al_2O_3$ ,  $TiO_2$  clay membrane (M5) at pH = 4, 7 and 9.

Fig. 5. The curve of uptake % of arsenic ions versus time at 10.0 mg/L  $As^{3+}$  for pH = 4, 7 and 9 is drawn in Fig. 6.

### 3.8. Effect of lead and arsenic ions concentration

The effect of lead and arsenic ions concentration on the uptake % of lead and arsenic on the PVDF/ $Al_2O_3$ ,  $TiO_2$  clay membrane (M5) was studied at constant pH Fig. 7 showed the effect of lead concentration (4.0 and 10.0 mg/L) on the uptake % of lead adsorbed from nitrate solution at constant pH (4) by the membrane. According to the diagram in Fig. 7, the uptake % of lead in concentrations of 4.0 and 10.0 mg/L is 63 and 88.5%, respectively. Fig. 8 shows the uptake % of arsenic adsorbed from nitrate solution at constant pH (7) in different concentrations of arsenic (4.0 and 10.0 mg/L). Also, the results showed that the uptake % of arsenic adsorption by the polymer membrane in concentrations of 4.0 and 10.0 mg/L is 74.5% and 91.0%, respectively.

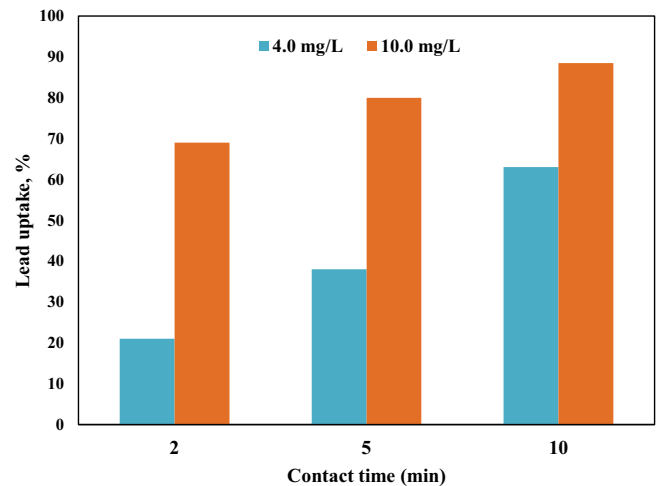


Fig. 7. Effect of lead concentration on the uptake % at pH 4.

Table 6

Comparisons of the performance of M5 membrane with other reported membranes

Membrane	Metal ion	Uptake %	Contact time (min)	pH	References
Magnetic nanoparticles impregnated chitosan beads	As(III)	96.0	300	6.8	[43]
	As(V)	96.0	300	6.8	
P-tert-butyl calix[8]areneoctamide impregnated Amberlite XAD-4 MTCC sawdust/ $MnFe_2O_4$ composite	As(V)	99.0	–	4.0	[44]
	As(III)	66.3	–	7.0	[45]
Alkyl(aliphatic)resorcinarene impregnated resin	Pb(II)	95.0	180	4.0	[46]
	Thiacalix[4]arene-loaded resin	Pb(II)	94.0	–	6.0
Bon powder	Pb(II)	96.0	120	4.0	[17]
Carbon active	Pb(II)	89.0	120	4.0	[17]
Commercial carbon	Pb(II)	50.0	120	4.0	[17]
Carboxyphenyl[1]resorcinarene impregnated resin	Pb(II)	99.7	60	6.5	[48]
Hydroxyapatite/ $NaP$ nanocomposite	Pb(II)	95.0	120	5.0	[49]
PVDF/ $ZnO$	Cu(II)	83.4	120	6.0	[28]
PVDF/ $Al_2O_3$ , $TiO_2$ clay (M5)	Pb(II)	88.5	10	4.0	This work
	As(III)	91.0	10	7.0	

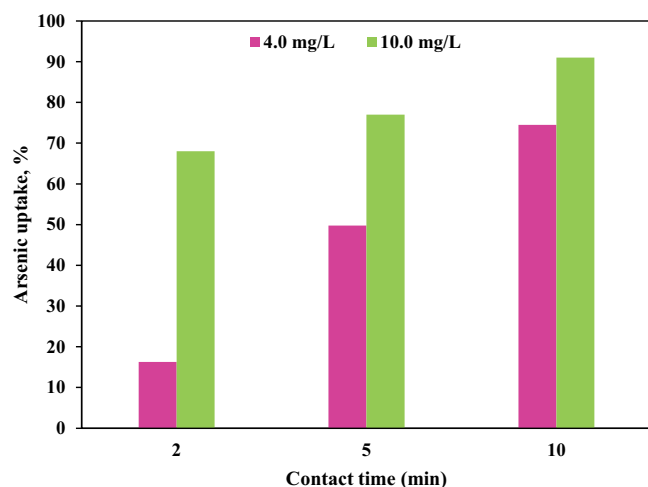


Fig. 8. Effect of arsenic concentration on the uptake % at pH 7.

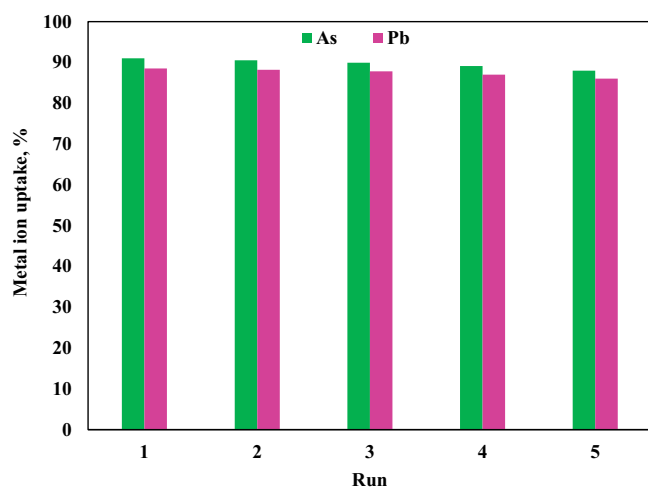


Fig. 9. Diagram of 5 cycles reuse of the membrane for absorption of lead (at pH = 4) and arsenic (at pH = 7) metal ions (contact time of 10 min, initial concentration of 10.0 mg/L).

The lead and arsenic uptake % are increased by increasing the concentration of lead and arsenic (10.0 mg/L).

Also, the comparisons of the performance of PVDF/ $\text{Al}_2\text{O}_3$ ,  $\text{TiO}_2$ , clay membrane (M5) with other reported membranes for removal of toxic metals (As and Pb) shows, in this work, the condition of adsorption (contact time of membrane, pH and uptake %) is very mild and ecofriendly (Table 5) [17,28,43–48].

### 3.9. Reusability of the membrane

The reusability experiments were also conducted on PVDF/ $\text{Al}_2\text{O}_3$ ,  $\text{TiO}_2$ , clay membrane (M5) and the results are shown in Fig. 9. The results show that the uptake % reduced about 1.0% in each run. Fig. 9 shows the diagram of 5 cycles of reuse of the membrane for adsorption of lead and arsenic metal ions. The uptake % of membrane could retain about 88.0 and 86.0% of the original adsorption capacity for As(III) and Pb(II), respectively, after 5 cycles of reuse.

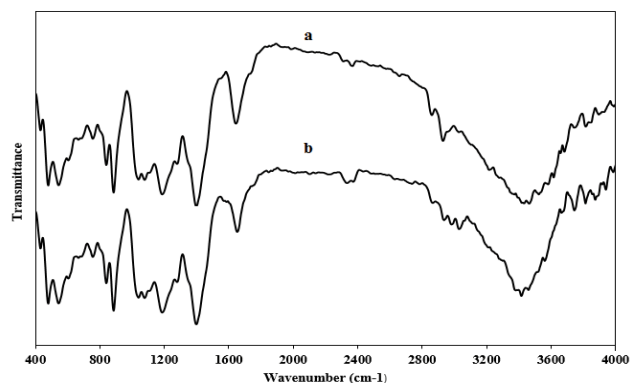


Fig. 10. Fourier-transform infrared spectra of fresh PVDF/ $\text{Al}_2\text{O}_3$ ,  $\text{TiO}_2$ , clay membrane (M5) (a) and after 5 runs using for removal of lead ions (b).

We considered the FT-IR of the membrane before and after 5 cycles of reuse. The FT-IR spectra show that there aren't any changes in the structure of the membrane after 5 runs (Fig. 10).

## 4. Conclusions

Organic–inorganic PVDF/ $\text{Al}_2\text{O}_3$ ,  $\text{TiO}_2$ , clay hybrid membranes were prepared and characterized. The addition of the nanosized  $\text{Al}_2\text{O}_3$ ,  $\text{TiO}_2$ , clay particles to the polymer did not affect membrane pore sizes and numbers, only by improving its surface hydrophilicity to improve many other properties of the membrane. The permeation increase of the membrane is attributed to surface hydrophilicity increase due to the hydrophilic inorganic nano-sized  $\text{Al}_2\text{O}_3$ ,  $\text{TiO}_2$ , clay particles addition. The results showed that, compared with PVDF membrane, the PVDF/ $\text{Al}_2\text{O}_3$ ,  $\text{TiO}_2$ , clay hybrid membrane (M5) showed better adsorption properties for lead and arsenic ions. The optimal conditions for lead ion adsorption (88.5%) was at pH 4, contact time of 10 min, and initial Pb(II) concentration equal to 10.0 mg/L. This membrane had remarkable efficiency for the sorption of As(III) (91.0%) from aqueous solutions; it was optimal at pH 7, contact time of 10 min, and initial Pb(II) concentration equal to 10.0 mg/L. Another important point is the very low dosage of nanoparticles ( $\text{Al}_2\text{O}_3$ ,  $\text{TiO}_2$ , and clay) inside the polymer tissue, which is very valuable from the point of view of green and economic chemistry compared to other adsorbents. This is because the dosage of titanium oxide nanoparticles in the polymer tissue is very low and about 1.0% by weight, it cannot be compared with other polymer adsorbents that contain a high percentage by weight of nanoparticles. Polar Ti–O bonds in  $\text{TiO}_2$  nanoparticles give them a high level of surface activity and the ability to act as adsorption carriers.  $\text{TiO}_2$  will polarize and produce a lot of hydroxyl groups due to ionization after absorbing water.

## Acknowledgment

Thanks to the Water and Environmental Research Centre, Shoushtar Branch, Islamic Azad University and the Fisheries Center, Agricultural Jihad Center and Imam



Khomeini Agriculture and Industry Company of Khuzestan province for supporting of this work.

## References

- [1] Z.H. Lu, G.J. Liu, S. Duncan, Poly(2-hydroxyethyl acrylate-co-methyl acrylate)/SiO<sub>2</sub>/TiO<sub>2</sub> hybrid membranes, *J. Membr. Sci.*, 221 (2003) 113–122.
- [2] C.H. Guizard, A. Bac, M. Barboiu, Hybrid organic-inorganic membranes with specific transport properties: applications in separation and sensors technologies, *Sep. Purif. Technol.*, 25 (2001) 167–180.
- [3] A. Taniguchi, M. Cakmak, The suppression of strain induced crystallization in PET through submicron TiO<sub>2</sub> particle incorporation, *Polymer*, 45 (2004) 6647–6654.
- [4] P.C. Chiang, W.T. Whang, M.H. Tsai, S.C. Wu, Physical and mechanical properties of polyimide/titania hybrid films, *Thin Solid Films*, 447 (2004) 359–364.
- [5] C. Garcia, E. Rogel-Hernández, S.W. Lin, H. Espinoza-Gómez, Natural organic matter fouling using a cellulose acetate copolymer ultrafiltration membrane, *Desal. Water Treat.*, 1 (2009) 150–156.
- [6] H. Dong, K.J. Xiao, X.L. Li, Y. Ren, S.Y. Guo, Preparation of PVDF/Al<sub>2</sub>O<sub>3</sub> hybrid membrane via the sol-gel process and characterization of the hybrid membrane, *Desal. Water Treat.*, 51 (2013) 3685–3690.
- [7] L. Sauguet, C. Boyer, B. Ameduri, B. Boutevin, Synthesis and characterization of poly(vinylidene fluoride)-*g*-poly(styrene) graft polymers obtained by atom transfer radical polymerization of styrene, *Macromolecules*, 39 (2006) 9087–9101.
- [8] L. Yan, Y.S. Li, C.B. Xiang, S. Xianda, Effect of nano-sized Al<sub>2</sub>O<sub>3</sub>-particle addition on PVDF ultrafiltration membrane performance, *J. Membr. Sci.*, 276 (2006) 162–167.
- [9] X.C. Cao, J. Ma, X.H. Shi, Z.J. Ren, Effect of TiO<sub>2</sub> nanoparticles size on the performance of PVDF membrane, *J. Appl. Surf. Sci.*, 253 (2006) 2003–2010.
- [10] A. Bottino, G. Capannelli, A. Comite, Preparation and characterization of novel porous PVDF-ZrO<sub>2</sub> composite membranes, *Desalination*, 146 (2002) 35–40.
- [11] L.Y. Yu, Z.L. Xu, H.M. Shen, H. Yang, Preparation and characterization of PVDF-SiO<sub>2</sub> composite hollow fiber UF membrane by sol-gel method, *J. Membr. Sci.*, 337 (2009) 257–265.
- [12] J.W. Cho, K.I. Sul, Characterization and properties of hybrid composites prepared from poly(vinylidene fluoride-tetrafluoroethylene) and SiO<sub>2</sub>, *Polymers*, 42 (2001) 727–736.
- [13] R.A. Zoppi, C.G.A. Soares, Hybrids of poly(ethylene oxide-*b*-amide-6) and ZrO<sub>2</sub> sol-gel: preparation, characterization, and application in processes of membrane separation, *Adv. Polym. Technol.*, 21 (2002) 2–16.
- [14] J.H. Kim, Y.M. Lee, Gas permeation properties of poly(amide-6-*b*-ethylene oxide)-silica hybrid membranes, *J. Membr. Sci.*, 193 (2001) 209–225.
- [15] I. Zawierucha, C. Kozlowski, G. Malin, Immobilized materials for removal of toxic metal ions from surface/groundwaters and aqueous waste streams, *Environ. Sci. Processes Impacts*, 18 (2016) 429–444.
- [16] L. Yan, Y.S. Li, C.B. Xiang, Preparation of poly(vinylidene fluoride) (PVDF) ultrafiltration membrane modified by nano-sized alumina (Al<sub>2</sub>O<sub>3</sub>) and its antifouling research, *Polymers*, 46 (2005) 7701–7706.
- [17] S.H. Abdel-Halim, A.M.A. Shehata, M.F. El-Shahat, Removal of lead ions from industrial wastewater by different types of natural materials, *Water Res.*, 37 (2003) 1678–1683.
- [18] M. Nakada, K. Fukaya, S. Takeshita, Y. Wadd, The accumulation of heavy metals in the submerged plants (*Elodea nuttallii*), *Bull. Environ. Contam. Toxicol.*, 22 (1979) 21–26.
- [19] D.L. Tsalev, Z.K. Zaprianov, AAS in Occupational and Environmental Health Practice, 2nd ed., CRC Press, Boca Raton, FL, 1985, p. 109.
- [20] T. Maruyama, S.A. Hannah, J.M. Cohen, Metals removal by physical and chemical treatment processes, *J. Water Pollut. Contam. Fed.*, 47 (1975) 962–975.
- [21] K.H. Park, M.A. Park, H. Jang, E.K. Kim, Y.H. Kim, Removal of heavy metals, cadmium II and lead II ions in water by *Sargassum herneri*, *Anal. Sci. Technol.*, 12 (1999) 196–202.
- [22] D. Petruzzelli, M. Pagano, G. Triavanti, R. Passino, Lead removal and recovery from battery waste waters by natural zeolite clinoptilolite, *Solvent Extr. Ion Exch.*, 17 (1999) 677–694.
- [23] H. Faghihian, M. Ghannadi-Marageh, H. Kazemian, The use of clinoptilolite of radioactive cesium and strontium from nuclear wastewater and lead, nickel, cadmium, barium from municipal wastewater, *Sep. Sci. Technol.*, 34 (1999) 2275–2292.
- [24] A. Vecchio, C. Finoli, D. Di-Simine, V. Andreoni, Heavy metal biosorption by bacterial cells, *Fresenius J. Anal. Chem.*, 361 (1998) 338–342.
- [25] R.K. Srivastav, S.K. Gupta, K.D.P. Nigam, P. Vasudevan, Use of aquatic plants for the removal of heavy metals from waste waters, *Int. J. Environ. Stud.*, 45 (1993) 43–50.
- [26] C. Namasivayam, K. Ranganathan, Removal of Cd(II) from waste water by adsorption on waste FeIII/CrIII hydroxide, *Water Res.*, 29 (1995) 1737–1744.
- [27] M.T. Laumakis, P.J. Martin, S. Pamucku, K. Owens, Proceeding of the International Conference on Hazard Waste Management, ASCE, New York, 1995, pp. 528–535.
- [28] X. Zhang, Y. Wang, Y. Liu, J. Xu, Y. Han, X. Xu, Preparation, performances of PVDF/ZnO hybrid membranes and their applications in the removal of copper ions, *Appl. Surf. Sci.*, 316 (2014) 333–340.
- [29] X. Sun, H. Shiraz, R. Wong, J. Zhang, J. Liu, J. Lu, N. Meng, Enhancing the performance of PVDF/GO ultrafiltration membrane via improving the dispersion of GO with homogeniser, *Membranes*, 12 (2022) 1268, doi: 10.3390/membranes12121268.
- [30] Y. Zhang, Y. Hu, Y. Zhang, S. Liu, TiO<sub>2</sub>/void/porous Al<sub>2</sub>O<sub>3</sub> shell embedded in polyvinylidene fluoride film for cleaning wastewater, *Adv. Powder Technol.*, 29 (2018) 1582–1590.
- [31] D. Wei, S. Zhou, M. Li, A. Xue, Y. Zhang, Y. Zhao, J. Zhong, D. Yang, PVDF/palygorskite composite ultrafiltration membranes: effects of nano-clay particles on membrane structure and properties, *Appl. Clay Sci.*, 181 (2019) 105171, doi: 10.1016/j.clay.2019.105171.
- [32] X.S. Yi, W.X. Shi, S.L. Yu, C. Ma, N. Sun, S. Wang, L.M. Jin, L.P. Sun, Optimization of complex conditions by response surface methodology for APAM-oil/water emulsion removal from aqua solutions using nano-sized TiO<sub>2</sub>/Al<sub>2</sub>O<sub>3</sub> PVDF ultrafiltration membrane, *J. Hazard. Mater.*, 193 (2011) 37–44.
- [33] R. Gregorio, R.C. Capitaio, Morphology and phase transition of high melt temperature crystallized poly(vinylidene fluoride), *J. Mater. Sci.*, 35 (2000) 299–306.
- [34] A. Salimi, A.A. Yousefi, FT-IR studies of β-phase crystal formation in stretched PVDF films, *Polym. Test.*, 22 (2003) 699–704.
- [35] T. Bocaccio, A. Bottino, G. Capanelli, P. Piaggio, Characterization of PDVF membranes by vibrational spectroscopy, *J. Membr. Sci.*, 210 (2002) 315–329.
- [36] M.A. Qing, Synthesis of alumina-silicon dioxide nano powders via sol-gel process, *J. Nat. Univ. Defense Technol.*, 24 (2002) 25–28.
- [37] T. Ogoshi, Y. Chujo, Synthesis of poly(vinylidene fluoride) (PVDF)/silica hybrids having interpenetrating polymer network structure by using crystallization between PVDF chains, *J. Polym. Sci., Part A: Polym. Chem.*, 43 (2005) 3543–3550.
- [38] W. Li, H. Li, Y.M. Zhang, Preparation and investigation of PVDF/PMMA/TiO<sub>2</sub> composite film, *J. Mater. Sci.*, 44 (2009) 2977–2984.
- [39] F. Tibi, S.J. Park, J. Kim, Improvement of membrane distillation using PVDF membrane incorporated with TiO<sub>2</sub> modified by silane and optimization of fabricating conditions, *Membr. J.*, 11 (2021) 1–18.
- [40] L. Huang, J.T. Arena, J.R. McCutcheon, Surface modified PVDF nanofiber supported thin film composite membranes for forward osmosis, *J. Membr. Sci.*, 499 (2016) 352–360.
- [41] X. Yue, X. Ji, H. Xu, B. Yang, M. Wang, Y. Yang, Performance investigation on GO-TiO<sub>2</sub>/PVDF composite ultrafiltration

- membrane for slightly polluted ground water treatment, *Energy*, 273 (2023) 127215, doi: 10.1016/j.energy.2023.127215.
- [42] W. Xie, W. Song, J. Li, X. Zhang, W. Dong, F. Sun, Micro-polluted water resources treatment by PVDF-TiO<sub>2</sub> membrane combined with Fe<sup>2+</sup>/sodium dithionite (DTN)/O<sub>2</sub> pre-oxidation process, *Chemosphere*, 311 (2023) 136998, doi: 10.1016/j.chemosphere.2022.136998.
- [43] J. Wang, W. Xu, L. Chen, X. Huang, J. Liu, Preparation and evaluation of magnetic nanoparticles impregnated chitosan beads for arsenic removal from water, *Chem. Eng. J.*, 251 (2014) 25–34.
- [44] I. Qureshi, S. Memon, M. Yilmaz, An excellent arsenic(V) sorption behavior of p-tert-butylcalix[8]areneoctamide impregnated resin, *C.R. Chim.*, 13 (2010) 1416–1423.
- [45] M.S. Podder, C.B. Majumder, Fixed-bed column study for As(III) and As(V) removal and recovery by bacterial cells immobilized on sawdust/MnFe<sub>2</sub>O<sub>4</sub> composite, *Biochem. Eng. J.*, 105 (2016) 114–135.
- [46] I. Zawierucha, C. Kozłowski, G. Malina, Removal of toxic metal ions from landfill leachate by complementary sorption and transport across polymer inclusion membranes, *Waste Manage.*, 33 (2013) 2129–2136.
- [47] X. Hu, Y. Li, Y. Wang, X. Li, H. Li, X. Liu, P. Zhang, Adsorption kinetics, thermodynamics and isotherm of thiacalix[4]arene-loaded resin to heavy metal ions, *Desalination*, 259 (2010) 76–83.
- [48] I. Zawierucha, J. Kozłowska, C. Kozłowski, A. Trochimczuk, Sorption of Pb(II), Cd(II) and Zn(II) performed with the use of carboxyphenylresorcinarene-impregnated Amberlite XAD-4 resin, *Desal. Water Treat.*, 52 (2014) 314–323.
- [49] M. Zendejdel, B. Shoshtari-Yeganeh, G. Cruciani, Removal of heavy metals and bacteria from aqueous solution by novel hydroxyapatite/zeolite nanocomposite, preparation and characterization, *J. Iran. Chem. Soc.*, 13 (2016) 1915–1930.